

TABLE 1

$V_{cp}$ volts	5				10				20			
$E, V/cm$	$4 \cdot 10^6$	$8 \cdot 10^6$	$1,6 \times 10^7$	$3,2 \times 10^7$	$4 \cdot 10^6$	$8 \cdot 10^6$	$1,6 \times 10^7$	$3,2 \times 10^7$	$4 \cdot 10^6$	$8 \cdot 10^6$	$1,6 \times 10^7$	$3,2 \times 10^7$
$R$	6,2	3,1	1,55	0,77	25	12,5	6,2	3,1	100	50	25	12,5

In conclusion, we note that, for temperatures above  $2500^\circ K$  and fields  $F < 5 \cdot 10^7$  V/cm, the fraction of electrons overcoming the potential barrier as a result of the tunnel effect is considerably less than the fraction of electrons passing over the barrier  $J_{I-F-T}$ . For temperatures below  $2500^\circ K$  and fields of  $(3-5) \cdot 10^7$  V/cm, the current density can attain  $J_{I-F-T}$  and then, with a rise in the field, can considerably exceed  $J_{I-T-F}$ .

With a transition from an I-T-F- to an I-F-T-emission, the point of inflection on the curves is almost not visible, while, with a transition from a T-F- to an F-T-emission, there is a sharp point of inflection with fields of  $\sim 4 \cdot 10^7$  V/cm, where the tunnel effect begins to be strongly felt. The effect of the discrete character of the distribution of the charge in the precathode layer rises with a rise in the precathode potential for I-T-F- and I-F-T-emissions, which is connected with a rise in the dimensionless parameter  $R = nd^3$ .

## LITERATURE CITED

1. E. Guth and J. Mullin, "The transition from thermionic to cold emission," *Phys. Rev.*, **61**, 339 (1942).
2. V. I. Rakhovskii, *Physical Principles of the Commutation of an Electrical Current in a Vacuum* [in Russian], Nauka, Moscow (1970).
3. I. N. Ostretsov, V. A. Petrosov, A. A. Porotnikov, and B. B. Rodnevich, "The equation of thermionic emission to a plasma," *Zh. Prikl. Mekh. Tekh. Fiz.*, No. 3 (1972).
4. A. A. Porotnikov and B. B. Rodnevich, "Thermoemission taking account of individual ionic fields," *Zh. Tekh. Fiz.*, **46**, No. 6 (1976).
5. A. A. Porotnikov and B. B. Rodnevich, "Autoemission taking account of individual ionic fields," *Zh. Tekh. Fiz.*, **46**, No. 10 (1976).
6. I. N. Ostretsov, V. A. Petrosov, A. A. Porotnikov, and B. B. Rodnevich, "The effect of individual ionic fields on the emission characteristics of thermocathodes," *Zh. Tekh. Fiz.*, **43**, No. 8 (1973).

CHARACTERISTICS OF A TWO-STAGE ION ACCELERATOR  
WITH AN ANODE LAYER

S. D. Grishin, V. S. Erofeev,  
A. V. Zharinov, V. P. Naumkin,  
and I. N. Safronov

UDC 629.7.036.74

Introduction

Plasma accelerators with a closed Hall current [1] are now undergoing ever greater development. From the macroscopic point of view the acceleration of plasma in these devices is accomplished by the electromagnetic force produced by the interaction of the Hall current with the external magnetic field. The concrete mechanism of the manifestation of this force consists in the fact that if the electrons are magnetized, then an electric field can be created in the plasma which accelerates the ions, whereas the electrons are forced to drift in the direction of the vector  $[\mathbf{E} \times \mathbf{H}]$ . If the conditions are uniform in the direction of the drift, then the drift or Hall current which develops closes on itself and the necessity of its commutation drops out.

Great attention is paid to one modification of an accelerator with closed drift: an accelerator with an extended acceleration zone and with dielectric walls for the accelerator chamber [2-6]. This system has been studied since the start of the 1960s. Serious development of another modification - an accelerator with an anode layer, most easily formed above metal cathode walls - began somewhat later, although the principle of

Kaliningrad, Moscow, Oblast. Translated from *Zhurnal Prikladnoi Mekhaniki i Tekhnicheskoi Fiziki*, No. 2, pp. 28-36, March-April, 1978. Original article submitted December 29, 1976.

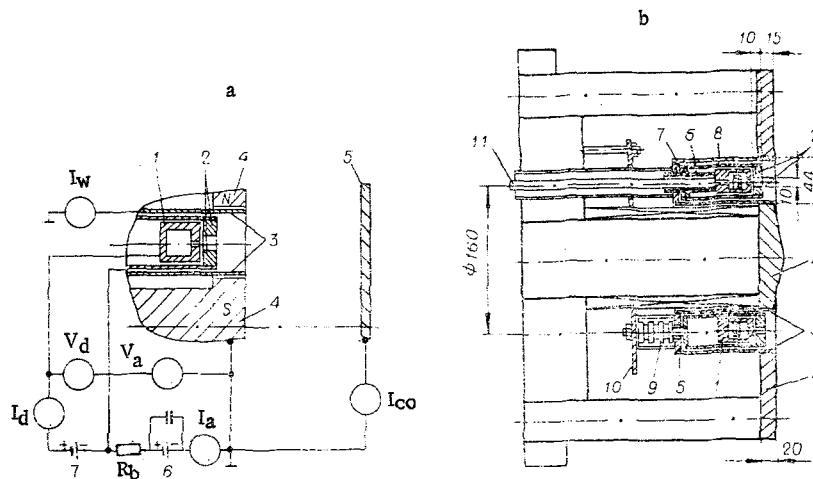


Fig. 1

an accelerator with a closed Hall current was itself proposed first, evidently in the very form of the acceleration of ions in the anode layer [7].

The extent of the acceleration zone, i.e., the region where the main drop in the applied potential difference occurs, in an accelerator with a closed Hall current can be estimated from the equation of balance of the creation of electrons and their departure from the volume. If the mobility of the electrons across the magnetic field is close to the classical value, then the potential drop proves to be concentrated near the anode in a layer with a thickness [8-10]

$$d \approx \frac{\sqrt{\frac{2e}{m} V_a}}{\omega_e} \sqrt{\frac{\nu_0}{\nu_i}} \approx \rho_e \sqrt{\frac{\nu_0}{\nu_i}},$$

where  $\omega_e$  is the electron cyclotron frequency;  $m$  and  $e$  are the electron mass and charge;  $V_a$  is the potential drop in the layer; and  $\nu_0$  and  $\nu_i$  are the frequencies of electron collisions with scattering of the momentum and of ionizations.

The simplest case of the existence of an anode layer occurs in the low-pressure discharge in a Penning cell and in direct and reverse magnetron cells [11, 12]. The formation of a layer in a plasma in the presence of a significant flow of ions was shown experimentally in [7]. A study of the formation of ion beams in an anode layer with a closed Hall current was carried out on an ion magnetron in [13], where the unique possibilities of the layer were confirmed. Preliminary results of a study of an axial accelerator with an anode layer (AAL) are presented in [14, 15]. The results of a detailed study of such an accelerator are laid out in the present report.

## 1. Description of the Construction and Experimental Conditions

In the creation of an axial accelerator with an anode layer, one of the main difficulties was the problem of the annular ion source. In practice, the use of surface ionization for this purpose restricts the choice of the working substance to cesium alone, and it is associated with the solution of difficult technological problems. Gas-discharge ion sources are more versatile. The use of an auxiliary EH-discharge with a closed Hall current as the ion source and the creation of a two-stage axial accelerator [14, 15] are evidently the most promising.

A schematic diagram of an axial two-stage ion accelerator is presented in Fig. 1a. The first stage (the discharge chamber or ion source) consists of the anode-vapor distributor 1 and the annular cathodes 2. The latter are simultaneously the anodes for the second stage and, together with the cylindrical screens 3, form the second stage (the accelerator chamber). Both stages (we call them the electrode assembly) are located in the annular gap of the magnetic system 4 (with poles N and S) which creates a radial magnetic field. The ion beam is received by the water-cooled current collector 5. The rectifiers 6 and 7 serve as the sources for the accelerating and discharge voltages.

Bismuth was chosen as the working substance for an experimental study of the accelerator under laboratory conditions. Condensing metals such as bismuth, lead, thallium, mercury, and cesium have an advantage

over gases, since they do not require a high-performance vacuum system. This advantage becomes decisive at large flow rates and justifies the difficulties caused by the necessity of maintaining the elements of the accelerator assembly at a high enough temperature. Among the enumerated metals preference was given to bismuth as the least toxic.

The construction of the bismuth axial accelerator, designed for a power of up to  $\sim 150$  kW, is shown schematically in Fig. 1b. The poles 4 forming the magnetic field are cooled in order to prevent their overheating from the power emitted by the electrode assembly. The solenoid winding is located on the central core of the magnetic circuit. The outer magnetic circuit is made of four rods. The field strength along the central diameter of the working gap of the magnetic system varies from 0 to 2 kOe. Henceforth all values of the strength are given for the central diameter.

The walls 3 of the accelerator chamber consist of two coaxial cylinders fastened to the flange 5. The anode-vapor distributor 1 is fastened to the flange 7 through the discharge insulators 6. The cathodes 2 of the first stage are also mounted on it with the help of the cylinders 8. The discharge chamber is mounted on the intermediate flange 10, which joins to the magnet, with the high-voltage insulators 9, while the accelerator chamber is mounted on it with metal bolts. The gap between the anode-vapor distributor and the cathodes is about 1 mm, while that between the cylindrical surfaces of the anode and the walls of the first and second stages is  $\sim 2$  mm. The bismuth vapor enters the vapor distributor through the vapor pipe 11 from the supply system.

The anode-vapor distributor must provide a uniform supply of bismuth vapor along the perimeter into the discharge cavity between the cathodes. For this there are 180 uniformly distributed openings in the cover of the anode. Since the bismuth enters the anode at one point, to assure the azimuthal uniformity of the supply the dimensions of its inner cavity must be such that the gasdynamic conduction along the perimeter is much greater than the total conduction of all the exit openings. When the diameter of the openings is 0.8 mm and the channel length is 3 mm the calculated pressure in the vapor distributor is  $\sim 2$  mm Hg for a flow rate of 22 mg/sec (10 A), which corresponds to a temperature of about  $1000^\circ\text{C}$  for the saturated bismuth vapor. A graphite heater is used to heat the anode to this temperature. The heater is located inside the anode, which assures its high efficiency. The remaining components of the electrode assembly are heated through the emission of the anode. All the metal components of the assembly are made of molybdenum, while the insulators are made of pure aluminum oxide. The most energy-stressed elements are the cathodes of the first stage, since they collect the energy brought in by the electrons of the accelerating layer.

As a rule, the electrode assembly is located in the magnetic system in such a way that the accelerating layer lies in the working gap where the magnetic field strength is greatest while the curvature of the magnetic field lines is slight. This makes it possible, without particular difficulties, to match the plane and surfaces of the two anodes facing the accelerating layer with the magnetic field lines and with each other. In the case of misalignment of the anodes relative to each other or relative to the magnetic field lines, all the electrons from the layer are "intercepted" by the sections of anode protruding in the direction perpendicular to  $H$  [11]. Local overheating occurs in these sections, which can lead to melting of the anode at a sufficiently high power.

With such a placement of the accelerating chamber the discharge stage finds itself in the region of a declining magnetic field, which is favorable for an ion source, since a smaller magnetic field than for the acceleration is more suitable from the point of view of efficient ionization [10, 16].

In performing the experimental studies the accelerator was mounted on a special weighing device permitting the direct measurement of the reaction force produced by the ion beam. A pressure of  $(10^{-5}-10^{-4})$  mm Hg was maintained in the vacuum chamber. The self-compensation of the space charge of the ion beam through the ionization of the residual gas is possible at such a vacuum. The accelerator therefore operated quite stably without any special source of electrons in the flight space. A current collector for the beam with a diameter of  $\sim 0.8$  m was placed opposite the accelerator at a distance of  $\sim 1.5$  m.

Three-phase bridge rectifiers were used as the sources for the accelerating and discharge voltages. A ballast resistance of  $R_b \approx 50 \Omega$  was included in the circuit of the accelerating-voltage rectifier to limit the current during a short circuit or breakdowns. Its size does not have a significant effect on the operation of the accelerator. A special experiment showed that a decrease in  $R_b$  to zero changes its characteristics weakly. The capacitance  $C$  shunting the accelerating-voltage rectifier has more importance. Without this capacitance in the accelerator one observes intense breakdowns, greatly hindering the operation of the accelerator. The inclusion of a capacitance of several microfarads stabilizes the operation.

In the course of the experiments we usually measured the accelerating and discharge voltages  $V_a$  and  $V_d$ , the currents  $I_a$  and  $I_d$  in the rectifier circuits of the two stages, and the current  $I_{c0}$  to the collector. In a number of experiments we measured the current  $I_w$  to the walls of the accelerating chamber. The total flow rate

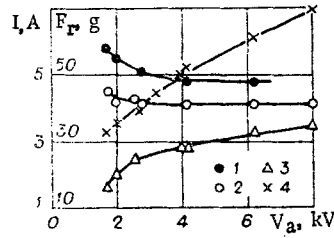


Fig. 2

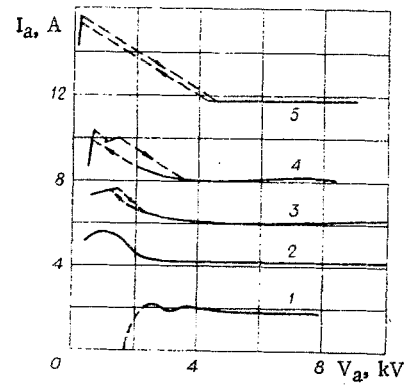


Fig. 3

of the working substance was measured by weighing the supply system before and after the experiments. This made it possible to determine the average flow rate of bismuth per second m.

The measured currents and voltages were recorded either with a loop oscillograph of type K-115 or with scaled instruments.

## 2. Main Integral Characteristics of the Accelerator

The first step in the study of the accelerator consisted in the determination of its statistical characteristics and the establishment of the limits of stable operation as a function of the main parameters: the accelerating and discharge voltages, the magnetic field in the gap, and the flow rate of the working substance.

The volt-ampere characteristic curves of the accelerating stage are presented in Figs. 2 and 3. In Fig. 2 the currents  $I_a$ ,  $I_d$ , and  $I_{CO}$  and the reaction force  $F_R$  of the beam are presented as functions of the accelerating voltage: 1)  $I_d$ ; 2)  $I_a$ ; 3)  $I_{CO}$ ; 4)  $F_R$ ;  $V_d = 150-370$  V,  $H = 2$  kOe. In Fig. 3 the current of the accelerating stage is given as a function of the voltage  $V_a$  at different flow rates of the working substance: 1)  $\dot{m} = 4.08$ ; 2) 9.25; 3) 13.1; 4) 17.4 mg/sec;  $V_d = 150$  V,  $H = 1.6$  kOe,  $p_{res} = (1.5-2) \cdot 10^{-5}$  mm Hg; 5)  $\dot{m} = 25.6$  mg/sec,  $V_d = 180$  V,  $H = 2$  kOe,  $p_{res} = 3 \cdot 10^{-5}$  mm Hg.

In the dependence of  $I_a$  on  $V_a$  (curves 3-5, Fig. 3) one can distinguish at least three different regions: a region of accelerating voltages where  $I_a$  hardly depends on  $V_a$ , a region with a negative slope of the volt-ampere characteristic curve, and a region of the low-voltage mode where  $I_a$  grows with an increase in  $V_a$ .

The AAL has the best parameters in the section of the dependence where  $I_a = \text{const}$  (the normal acceleration mode). In this mode the focusing of the beam improves with an increase in  $V_a$  and the current  $I_{CO}$  to the collector increases, approaching the current of the accelerating stage. In this mode  $I_a$  coincides with the bismuth flow rate per second  $\text{em}/M$  ( $M$  is the atomic mass) with the accuracy of the measurement error ( $\pm 5\%$ ). The current  $I_w$  to the wall of the accelerator chamber is negative, as a rule, and can comprise an appreciable value ( $\sim 0.1I_a$ ).

In the region with a negative slope the current to the collector decreases, the beam geometry deteriorates, and the current to the walls of the accelerator chamber changes sign from negative to positive, with the value of  $I_w$  reaching  $(0.3-0.5)I_a$ . One is not always able to trace this region; often an abrupt transition occurs from the acceleration mode to the low-voltage mode and vice versa. Curves taken with a decrease and with an increase in the accelerating voltage do not always coincide; "hysteresis" is observed as a rule. The low-voltage mode can be called anomalous from the point of view of the efficient organization of the acceleration process. In the majority of cases in this mode the current of the accelerating stage considerably exceeds the flow rate  $\text{em}/M$ , while the beam does not have a clearly expressed form.

The efficient operation of a two-stage accelerator starts with some minimum value of the flow rate below which the accelerator cannot operate. For the model investigated it comprises  $\sim 2$  A. With a further decrease in the flow rate the degree of ionization declines sharply and the current in both stages decreases by several orders of magnitude.

Such a sharp decline in the degree of ionization is in qualitative agreement with the theoretical concepts of [10], which say that efficient ionization in the anode layer occurs only at a sufficiently high flow rate of the working substance. A qualitative estimate shows, however, that in the experiment efficient ionization starts at a flux density of neutral gas from the anode ( $q_0 \approx 0.04$  A/cm<sup>2</sup>) several times lower than follows from [10].

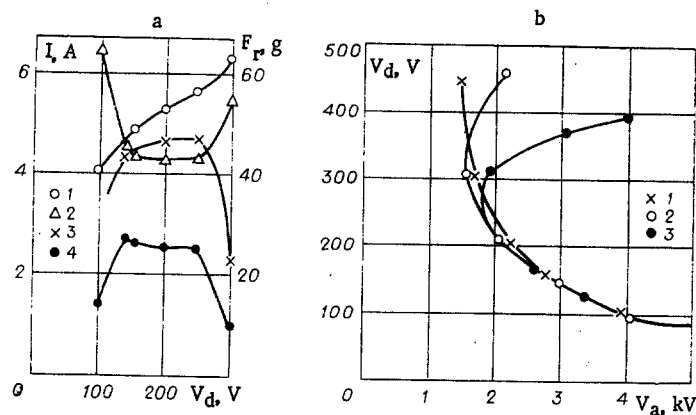


Fig. 4

Such a disagreement may be connected with the fact that in this estimate the total current (2 A) is referred to the entire surface of the anode lying between the cathodes (50 cm<sup>2</sup>). In reality, the delivery of gas to the discharge cavity takes place from the openings, so that the true density of the flux of neutral particles into the ionization zone is considerably higher than 0.04 A/cm<sup>2</sup>.

A comparison of the curves (see Fig. 3) indicates that the flow rate markedly modifies the volt-ampere characteristic curve in the region of low  $V_a$ . At low flow rates (curves 1 and 2)  $I_a$  varies smoothly with a decrease in  $V_a$  and the mode is stable. At high flow rates the region with a negative slope of the volt-ampere characteristic curve starts at higher  $V_a$  and the steepness increases. The mode becomes unstable and its abrupt change occurs (it is denoted by dashed lines in Fig. 3).

In the anomalous mode the volt-ampere characteristic curve has a rather complicated structure. It is traced most clearly in curve 4. Two branches with a positive slope are present, on which the accelerator operates stably, although it has poor output characteristics.

We discovered a peculiarity of the accelerator, manifested in the fact that at increased discharge voltages (250-300 V) there is a region of  $V_a$  in which intense breakdowns are observed. This region can be passed through by a further increase in the accelerating voltage. The existence of such a region is probably connected with the presence of the high-frequency oscillations accompanying the operation of an accelerator [17]. At higher flow rates, when the power required by the accelerator exceeds 80-100 kW, one is not able to "get through" the breakdown.

The maximum current of accelerated bismuth ions (presently obtained) is 14 A (density 0.28 A/cm<sup>2</sup>). A further increase in flow rate is limited by the capabilities of the electric power supply system.

The current of the discharge stage hardly depends on  $V_a$  in the region of the normal acceleration mode and grows upon a transition to the anomalous mode. In the acceleration mode the discharge current usually exceeds  $I_a$  by 1.2-1.3 times.

The range of discharge voltages in which an accelerator with an anode layer possesses the optimum characteristics is rather narrow. An example of the currents of both stages, the current to the collector, and the reaction force of the beam as functions of the discharge voltage is shown in Fig. 4a: 1)  $I_d$ ; 2)  $I_a$ ; 3)  $F_r$ ; 4)  $I_{CO}$ ;  $V_a = 3$  kV,  $H = 1.8$  kOe. One can distinguish a region in which the currents  $I_a$  and  $I_{CO}$  and the quantity  $F_r$  depend weakly on  $V_d$  while the current  $I_d$  of the first stage grows monotonically with an increase in  $V_d$ . The beam is well formed in this region. At its boundaries one observes a sharp increase in the current  $I_a$  and a collapse into the anomalous mode. The collapse is accompanied by defocusing of the beam and a sharp decrease in  $I_{CO}$  and  $F_r$ .

The working range of discharge voltages depends on the accelerating voltage and the flow rate. The dependence of the values of  $V_d$  corresponding to the boundaries of the region of the acceleration mode on the accelerating voltage at different flow rates of the working substance ( $e\dot{m}/M \approx I_a$  in the acceleration mode) is shown in Fig. 4b: 1)  $I_a = 2.6$ ; 2) 3.8; 3) 5 A;  $H = 1.8$  kOe. A decrease in the flow rate at a fixed  $V_a$  widens the range of discharge voltages with optimum characteristics of the accelerator, especially toward larger  $V_d$ . A decrease in  $V_a$  leads to narrowing of the region of stable operation with respect to the discharge voltage. At accelerating voltages of  $V_a \leq 1.5$  kV we could not obtain the normal acceleration mode on the test model at any values of  $V_d$  and the flow rate.

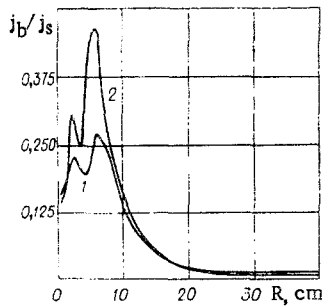


Fig. 5

In the experimental study of the AAL it was discovered that a sufficiently strong magnetic field is required to assure stable operation ( $H \approx 1$  kOe for  $I_a = 4$  A) [15]. This is an important property of a two-stage accelerator with an anode layer. The existence of a minimum magnetic field strength below which the acceleration mode changes into the anomalous mode is characteristic. This is preceded by an increase in the currents  $I_a$  and  $I_d$ . The strength at which the transition occurs increases with an increase in  $I_a$ .

A study of the parameters of the ion beam obtained in an accelerator with an anode layer is associated with certain difficulties, consisting in the fact that a powerful ion stream leads to the heating and rapid sputtering of any detection devices placed in it. Therefore, in the first stage the greatest attention was paid to the determination of the average velocity of the ions from the measured reaction force of the jet and average-mass flow rate, as well as to a study of the radial density distribution of the ion current with a movable detector. Figure 5 gives a concept of the radial density distribution of the ion current  $j_b$  in the beam, normalized to the current density  $j_s$  at the exit from the ion source, for two values of the accelerating voltage (distance from accelerator cut 12 cm): 1)  $V_a = 5$  kV; 2)  $V_a = 8.15$  kV;  $I_a = 4$  A,  $V_d = 180$  V,  $H = 1.8$  kOe. It is seen that the focusing of the beam improves with an increase in  $V_a$ . The complexity of the beam structure displayed (the presence of two maxima) requires the conducting of further experimental investigation for its interpretation.

An example of the dependence of the reaction force  $F_R$  of the beam of accelerated ions on the accelerating voltage is presented in Fig. 2, while the experimental dependence of  $F_R$  on the current  $I_a$  of accelerated ions is shown in Fig. 6a:  $V_d = 100$ – $200$  V,  $V_a = 4$  kV,  $H = 2$ – $3$  kOe. In the acceleration mode the value of  $F_R$  is connected linearly with  $I_a$  in the entire range of bismuth flow rate studied and is proportional to  $V_a^{1/2}$ . Therefore, the average-mass velocity  $\langle v_i \rangle$  of the ions depends only on the accelerating voltage and is approximately described by the relation

$$\langle v_i^{\text{exp}} \rangle \approx 2.7 \cdot 10^6 \sqrt{V_a},$$

where the velocity  $v_i$  is expressed in cm/sec and the voltage  $V_a$  in kV. The experimental dependence  $\langle v_i \rangle(V_a)$  is given in Fig. 6b (curve 1), where the theoretical curve 2 of  $\langle v_i \rangle_{\text{max}} = 3.05 \cdot 10^6 \sqrt{V_a}$  is also presented for the case when the ions acquire an energy corresponding to the total applied potential difference.

On the basis of the velocity obtained in the experiment, one can compute the efficiency of the accelerator ( $\eta_a$ , curve 3), equal to  $\sim 0.75$  for  $V_a = 4$  kV. As the accelerating voltage varies from 2 to 10 kV, the quantity  $\eta_a$  grows from  $\sim 0.6$  to  $\sim 0.8$  (see Fig. 6b). The increase in  $\eta_a$  is explained by the relative decrease in the fraction of the power expended on the obtainment of the ions and by the improvement of the beam focusing. The transition to the anomalous mode ( $V_a < 2$  kV) is accompanied by a sharp decline in the accelerator efficiency.

The results of the studies conducted indicate the unique possibilities of accelerators having an anode layer as a means of obtaining powerful ion beams. These possibilities are due to the fact that at high densities of the accelerated ion current the layer becomes quasineutral [9, 13], the density of the accelerated ion current

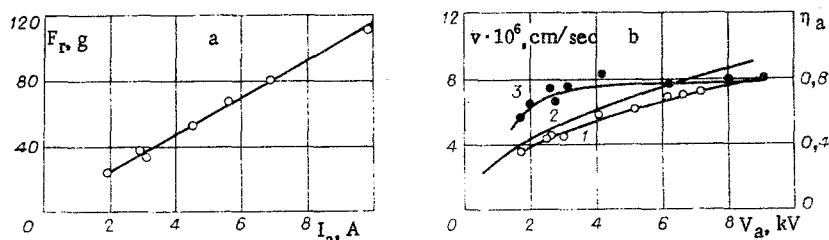


Fig. 6

is not space-charge limited, and it can be regulated within wide limits. In this respect an AAL is a plasma accelerator. At the same time, the short acceleration zone and the nondissipative mechanism of acceleration allow one to obtain ion beams with minimal losses, and AAL can compare with electrostatic ion accelerators, whose acceleration efficiencies are close to unity. The presently existing limit of the accelerating voltage at some minimum value is evidently connected not only with the properties of the layer but also with the conditions of the travel of the ion beam across the magnetic field [18, 19]. The question of how fundamental this limit is requires additional studies.

An accelerator with an anode layer can find application in the solution of a number of physico-technical problems, such as, for example, the following.

1. The creation of injectors for thermonuclear traps. According to theory [9, 10], the properties of the structure of the anode layer are determined in the first approximation by the space-charge density of the accelerated ion stream. From this point of view the AAL parameters obtained in the present work correspond to the formation of a proton beam with a current of  $\sim 100$  A.
2. The creation of engines for spacecraft [6]. Engines based on AAL should be promising, since such an accelerator permits regulation of the current and velocity of the ion beam in a wide range with retention of a high efficiency.
3. The use of ion beams in the technology of obtaining atomically pure surfaces, the doping of semiconductors, the obtaining of thin films by the method of cathode sputtering, etc. One can be confident that the use of AAL for these purposes will sharply increase the productivity of these processes.

#### LITERATURE CITED

1. Plasma Accelerators [in Russian], Mashinostroenie, Moscow (1972).
2. C. O. Brown and E. A. Pinsley, "Further experimental investigations of a cesium Hall-current accelerator," *AIAA J.*, **3**, 853 (1965).
3. G. S. Janes and R. S. Lowder, "Anomalous electron diffusion and ion acceleration in a low-density plasma," *Phys. Fluids*, **9**, No. 6, 115 (1966).
4. A. I. Morozov, Yu. V. Esipchuk, et al., "Influence of the magnetic field configuration on the operating mode of an accelerator with closed electron drift," *Zh. Tekh. Fiz.*, **42**, 612 (1972).
5. A. I. Morozov, A. Ya. Kislov, and I. P. Zubkov, "A high-current plasma accelerator with closed electron drift," *Pis'ma Zh. Tekh. Fiz.*, **7**, 224 (1968).
6. L. A. Artsimovich, I. M. Andronov, Yu. V. Esipchuk, et al., "Development of a steady plasma engine (SPE) and its testing on the Meteor earth satellite," *Kosm. Issled.*, **12**, No. 3, 451 (1974).
7. E. E. Yushmanov, "A radial potential distribution in a cylindrical magnetic trap with a magnetron means of ion injection," in: *Plasma Physics and the Problems of Controlled Thermonuclear Reactions* [in Russian], Vol. 4, Izd. Akad. Nauk SSSR, Moscow (1958).
8. Yu. S. Popov, "A Penning discharge with a cold cathode at a low pressure," *Zh. Tekh. Fiz.*, **37**, No. 1, 118 (1967).
9. A. V. Zharinov and Yu. S. Popov, "On plasma acceleration by a closed Hall current," *Zh. Tekh. Fiz.*, **37**, No. 2, 294 (1967).
10. V. S. Erofeev, Yu. V. Sanochkin, and S. S. Filippov, "The electrical anode layer in a discharge with a closed Hall current," *Zh. Prikl. Mekh. Tekh. Fiz.*, No. 5, 3 (1969).
11. N. A. Kervalishvili and A. V. Zharinov, "Characteristics of a low-pressure discharge in a transverse magnetic field," *Zh. Tekh. Fiz.*, **35**, No. 12, 2194 (1965).
12. W. Knauer, "Mechanism of the Penning discharge at low pressures," *J. Appl. Phys.*, **33**, No. 6, 2093 (1962).
13. V. S. Erofeev and A. V. Sharinov, "Ion acceleration in an EH-layer with a closed Hall current," in: *Plasma Accelerators* [in Russian], Mashinostroenie, Moscow (1972).
14. M. A. Abdyukhanov, S. D. Grishin, V. S. Erofeev, A. V. Zharinov, V. P. Naumkin, and I. N. Safronov, "A two-stage Hall ion accelerator with an anode layer," in: *Materials of the Second All-Union Conference on Plasma Accelerators* [in Russian], Izd. Inst. Fiz. Akad. Nauk BelorusSSR, Minsk (1973).
15. S. D. Grishin, V. S. Erofeev, L. V. Leskov, V. P. Naumkin, and I. N. Safronov, "Characteristics of a Hall ion accelerator with an anode layer," in: *Materials of the Second All-Union Conference on Plasma Accelerators* [in Russian], Izd. Inst. Fiz. Akad. Nauk BelorusSSR, Minsk (1973).
16. V. S. Erofeev, A. V. Zharinov, and E. A. Lyapin, "Two-stage ion acceleration in a layer with a closed Hall current," in: *Plasma Accelerators* [in Russian], Mashinostroenie, Moscow (1972).

17. V. S. Erofeev, K. P. Kirdyashev, and E. V. Pelepelin, "High-frequency oscillations in an accelerator with an anode layer," in: Materials of the Second All-Union Conference on Plasma Accelerators [in Russian], Izd. Inst. Fiz. Akad. Nauk BelorusSSR, Minsk (1973).
18. V. S. Erofeev, A. V. Zharinov, and E. A. Lyapin, "Low-frequency instability of a radial ion beam formed in an EH-layer with a closed Hall current," in: Plasma Accelerators [in Russian], Mashinostroenie, Moscow (1972).
19. A. V. Zharinov, "The amplitude of potential oscillations of a quasineutral ion beam," Pis'ma Zh. Tekh. Fiz., 17, No. 9, 508 (1973).

## DIAGNOSTICS OF SUPERSONIC TWO-PHASE STREAMS FROM SCATTERED LASER RADIATION

A. P. Alkhimov, V. M. Boiko,  
A. N. Papyrin, and R. I. Soloukhin

UDC 532.57+532.137+536.51+532.14.08+531.787

Further development of the experimental research technique is required for the solution of a wide circle of problems arising in the investigation of high-velocity two-phase flows and connected with the study of the physical processes of the interaction between particles and a nonequilibrium gas stream [1], such as in the nozzle of a solid-fuel rocket engine [2] (investigation of the effects of the velocity lag and thermal lag of the particles, determination of their sizes and coefficient of aerodynamic resistance, etc.). Here the most promising are noncontact optical methods of diagnostics, the intensity of whose development in recent years has been promoted by the extensive application of lasers. The laser Doppler velocity meter (LDVM), the determination of the disperse composition and particle concentration from the attenuation and scattering of a laser beam, and holographic and other methods have now been successfully incorporated into gasdynamic experimental practice.

The present report is devoted to the development of the laser Doppler velocity meter and the method of pulsed laser visualization for the investigation of high-velocity two-phase streams.

### The Laser Doppler Velocity Meter

It is known that LDVM systems can be divided into two main groups with respect to the means of measurement of the Doppler frequency shift of the scattered laser radiation. The first includes the most studied and widely distributed systems, in which the difference frequency is determined with the help of photodetectors (the photographic mixing method). A major cycle of research on the development of the theory and on the problems of the technical construction of such systems [the work of B. S. Rinkevichyus (Moscow Power Institute), V. S. Sobolev (Institute of Atomic Energy, Siberian Branch, Academy of Sciences of the USSR), G. L. Grodzovskii (Central Aerohydrodynamic Institute) and colleagues, and others] has contributed to the considerable progress in this field and has led to the creation of experimental models of instruments which have been used successfully in gasdynamic research. It should be noted, however, that from the point of view of practical realization these LDVM are simple enough in the measurement of relatively low velocities  $v \leq 10^2$  m/sec and are used most extensively and successfully in the study of subsonic streams, whereas the measurement of velocities  $v \geq 10^3$  m/sec by such a method presents considerable technical difficulties.

Of major interest on these grounds are the laser Doppler systems of the second class [3-9], which accomplish the direct measurement of the Doppler frequency shift with the help of high-resolution spectral instruments (such as the Fabry-Perot interferometer); at present they are still inadequately studied and are used considerably less often in gasdynamic research. These LDVM systems permit the practically unlimited expansion of the measurement range into the region of higher velocities and evidently are more promising for the investigation of supersonic and especially of hypersonic streams, since for the spectral recording method the reliability and accuracy of the measurements only increase with an increase in velocity.

In this connection it seemed desirable to conduct further research directed toward the development of laser Doppler systems of this type and, in particular, toward the creation of a scanning spectrometer having

---

Novosibirsk, Minsk. Translated from Zhurnal Prikladnoi Mekhaniki i Tekhnicheskoi Fiziki, No. 2, pp. 36-46, March-April, 1978. Original article submitted February 17, 1977.